Civil Engineering Infrastructures Journal, 52(2): 277 – 293, December 2019
Print ISSN: 2322-2093; Online ISSN: 2423-6691
DOI: 10.22059/ceij.2019.261794.1500

Reliability Assessment of Shallow Domes Using a Semi-Empirical Evaluation Procedure

Karimi, H.[1] and Mahmoudzadeh Kani, I.[2*]

[1] Ph.D. Candidate of Structural Engineering, School of Civil Engineering, College of Engineering, University of Tehran, Tehran, Iran.
[2] Professor of Structural Engineering, School of Civil Engineering, College of Engineering, University of Tehran, Tehran, Iran.

Received: 10 Jul. 2018; Revised: 29 Sep. 2019; Accepted: 13 Oct. 2019

ABSTRACT: Like other structures, shallow domes have imperfections from the prescribed values obtained by specifications during the construction process. Specifications define some tolerance values for imperfections. Despite consideration of these values, the critical load of a dome varies for each imperfection pattern. So the reliability plays an important role in domes safety. Theoretical evaluation procedure is the most accurate one to obtain reliability function, but it is only applicable to small structures. Semi-empirical evaluation procedure, on the other hand, is more implemented. In the present research reliability of real domes with stochastic initial imperfections has been investigated by comparing finite elements method, theoretical and semi-empirical results. Also, it has been shown that the automatic perturbed analysis is not sufficiently reliable for domes. So it is recommend that a suitable safety factor be applied on the automatic perturbed load or the method utilized in this paper be used to obtain the critical load – reliability diagram.

Keywords: Bifurcation, Finite Elements Method, Monte Carlo Method, Reliability, Shallow Domes.

INTRODUCTION

Shallow lattice domes due to their ease of installation and aesthetic appeal are useful and picturesque (Hassan, 2013; Liu and Ye, 2014). Considerable interest has been paid on the analysis and design of these structures by researchers and there has been much research about these domes in last decades (Heidari et al., 2019; Kani and Heidari, 2007; Karimi and Kani, 2019). But domes are more susceptible to unavoidable presence of both geometric and material nonlinearities (Kitipornchai and Al-Bermani, 1992; Kiyohiro and Kazuo, 1991). The existence of a bifurcation point which mainly aroused from the imperfection in material properties and geometrical configuration was a big problem. But nowadays by introducing the automatic perturbed analysis (Kani and Heidari, 2007) this problem has been resolved well. Although the problem has been well addressed, the safety of domes is still questioned. Despite the fact that many specifications and manufacturers documents have dictated tolerance for construction errors, different imperfection patterns may cause different critical load for the dome.

* Corresponding author E-mail: imkani@ut.ac.ir

Because uncertainties are the inventible companions of structural engineering design (Fröderberg and Thelandersson, 2015), they play an important role in the safety and the reliability of structures (Keshtegar and Miri, 2013). All aspects of uncertainties, however, cannot be recognized, but they can be treated in a safe manner. The critical load of shallow domes, like other structures, alters due to uncertainties. These alterations follow probability distribution functions varying from type to type of bifurcation. In the previous studies (Ikeda and Murota, 2010; Ikeda et al., 1996; Kiyohiro and Kazuo, 1993; Murota and Ikeda, 1992) theoretical form of the probability distribution and reliability functions for different types of bifurcation points had been derived. But using this form is not practical for the large scale domes due to high nonlinearity and computational costs. So another procedure was introduced (Kiyohiro and Kazuo, 1993) namely, the semi-empirical evaluation procedure. In this method approximations have been made to obtain some parameters from the empirical data. The most important parameter is the critical load of the dome and different material properties of the dome are from empirical data.

The critical load is obtained by the Finite Elements Method (FEM). FEM (Jensen et al., 2015; Kamiński and Świta, 2015) has been extensively applied to computational modeling to calculate the critical load. So in the work presented here by applying an in-house nonlinear FEM software, the critical load has been found. The aforementioned in-house software is a materially and geometrically combined nonlinear set of finite element analyses based on an incremental/iterative Newton–Raphson solution procedure (Karimi and Kani, 2019). This in-house software hereinafter is referred to as "CNASS". In CNASS, joints are modeled just as the fully rigid or the pin connections and other behavior of joints (such as the semi-rigid connections (Ramalingam and Jayachandran, 2015)) is not considered. Also, just static load combinations are used in CNASS, hence seismic loads (Nie et al., 2014) are not performed. Bifurcation points play an important role in the post-buckling behavior of domes (Moghaddasie and Stanciulescu, 2013). Tracing the post-buckling behavior of domes is one of the distinctive features of CNASS. It is worthwhile to note that the post-buckling behavior of shallow lattice domes is mainly studied based on an incremental manner (Abatan and Holzer, 1978).

Different material properties will be discussed and detailed in the following sections. Briefly, finite sets of random imperfection systems which are subject to the random distribution will be generated as initial parameters. This combination of FEM and random variables sometimes has been referred to as the stochastic finite element method (Kamiński and Świta, 2015; Liu et al., 2016) which itself is a branch of the Monte Carlo methods (Alvarez and Hurtado, 2014; Hurtado and Alvarez, 2013). Members material properties are part of the initial parameters. In the present method the code-based limits are used in order to make different material properties. In other words, the differences from the theoretical value in each imperfection mode (such as cross-sectional area) are under the permissible limits of variation dictated by codes.

Previously, the safety of structures had been studied based on deterministic values of the design parameters (Radoń, 2015), but nowadays, structural safety is ensured by reliability functions which are derived by numerical or experimental analyses. Due to the increasing number of designs based on reliability, in the present paper, the reliability functions of shallow lattice domes have been achieved with this approach. Although the focus of the present paper is on Live loads, it is possible to extend the study to many load

combinations with symmetry where some of these load combinations are described in Meimand and Schafer (2014).

Historically, the worst imperfection patterns causing the maximum change (decrease) of critical load have been determined by employing lots of Monte Carlo simulations (Ikeda and Murota, 2010). In these simulations computational cost is far more than the accuracy. Besides computational cost, a design based on the worst imperfection pattern is not economical at all. Because the possibility of such a pattern is very rare, it is recommended only for very special structures. It is thus necessary to use a more cost-effective method such as the reliability method for structural design of common structures.

Therefore, the reliability of shallow lattice domes with the stochastic finite element method has been investigated. In this regard, CNASS is used to compute the critical load corresponding to different imperfection patterns. Three examples have been investigated from simple structures to complicated one. Investigations on the behavior of simple structures are a basis for understanding the behavior of complicated structures (Akkas, 1976).

The present paper shows that using the automatic perfect perturbed analysis is not sufficient in itself and reliability analysis should be additionally performed applying the Monte Carlo method. The analytical method for finding the reliability function is more accurate. However, in many cases it is not applicable due to the highly nonlinear situation. Therefore, the semi-empirical method is used instead in the present work. As another outcome of this work, a safety factor for the critical load of dome is introduced by taking the reliability function into account. Without considering this safety factor, the dome may be at risk.

A brief outline of this paper is as follows. In section "Material and methods", some governing equations and characteristics of critical points are discussed. Section "Theory" reviews theory of stochastic properties of members and describes how to apply these properties into the model. Numerical results in section "Results and discussions" show the robustness and accuracy of the proposed method for various types of critical points. Finally, concluding remarks, notation and references have been presented.

MATERIAL AND METHODS

In the present work shallow domes are analyzed numerically by the method of Kani and Heidari (Kani and Heidari, 2007). To apply the method, a materially and geometrically nonlinear finite element code (CNASS) is used (Kani and Heidari, 2007).

A system of nonlinear equilibrium equations for a dome is considered (Ikeda et al., 1998):

$$\boldsymbol{F}(\lambda, \boldsymbol{u}, \vec{v}) = \boldsymbol{0} \tag{1}$$

where λ: interprets loading parameter, $\boldsymbol{u}$ and $\vec{v}$: are N- and p-dimensional vectors for nodal displacement and imperfection pattern, respectively. $\boldsymbol{F}$: is assumed sufficiently smooth and Jacobian of $\boldsymbol{F}$ (tangent stiffness matrix (Ghassemieh and Badrkhani Ajaei, 2018)) for the perfect system has no negative or zero eigenvalues. Equilibrium paths for a fixed $\vec{v}$ can be solved by the aforementioned system of equations. After solving the equilibrium path for each fixed $\vec{v}$ a set of λ_c and $\boldsymbol{u_c}$ could be obtained. Here λ_c denotes the critical point on the equilibrium path.

The imperfection vector $\vec{v}$ can be written as:

$$\vec{v} = \overrightarrow{v^0} + \varepsilon \vec{d} \tag{2}$$

where, $\vec{d}$: is the imperfection pattern vector and ε: denotes the magnitude of imperfection.

It is also noted that $\overrightarrow{v^0}$ and $\vec{v}$: are perfect and imperfect system vectors, respectively (Ikeda and Murota, 2010; Ikeda et al., 1996; Ikeda et al., 1998; Kiyohiro and Kazuo, 1991, 1993; Murota and Ikeda, 1992). To be more specific, an imperfection pattern is added to the nominal state of the system which is called the perfect system. In this notation, each component of $\vec{d}$,$d[i]$, defines one of the initial imperfections mode such as geometric configurations, material properties or cross-sectional area. In this paper, no geometrical imperfection is considered and just material properties such as modulus of elasticity and cross-sectional area are examined. Based on the report of steel profile manufacturers, the values of material properties are normal random variables (Taras and Huemer, 2015). In addition, the mean value of each property is its nominal one. In other words, $d[i]$, is normally distributed with mean value of zero.

On the other hand, most of specifications and manufacturers define imperfection limits for construction errors. Here, construction errors are identical to imperfection systems. Therefore, the below constraint is used.

$$|\varepsilon\, d[i]| \leq \Delta_{max} \tag{3}$$

where Δ_{max}: is a prescribed value obtained by specifications or manufacturers documents.

Theory for Simple Critical Points

Increment of the critical load in an imperfect system, $\tilde{\lambda}_c$, is introduced as Eq. (4) (Koiter, 1970).

$$\tilde{\lambda}_c = \lambda_c - \lambda_c^0 \sim C(\vec{d})\varepsilon^{\rho} \tag{4}$$

According to the type of bifurcation point $C(\vec{d})$ and ρ is determined as Eq. (5), if ε is sufficiently small.

$$\begin{cases} \rho = 1, & C(\vec{d}) = -C_0 a, & limit\ point \\ \rho = \dfrac{1}{2}, & C(\vec{d}) = -C_0 |a|^{\frac{1}{2}}, & asymmetric\ bifurcation\ point \\ \rho = \dfrac{2}{3}, & C(\vec{d}) = C_0 . a^{\frac{2}{3}}, & symmetric\ bifurcation\ point \end{cases} \tag{5}$$

where C_0: is a positive constant and may vary from type to type; a: depends on $\vec{d}$ and had been defined as $a \equiv \sum_{i=1}^{p} c_i d_i$ (Kiyohiro and Kazuo, 1993). If $\varepsilon\vec{d}$ is subjected to normal distribution with mean value of zero and the variance of $\tilde{\sigma}^2$, $N(0, \tilde{\sigma}^2)$, the following normalized value (Eq. 6) can be defined (Kiyohiro and Kazuo, 1993).

$$\tilde{a} = \frac{a}{\tilde{\sigma}}\ , \sigma = \tilde{\sigma}\varepsilon \tag{6}$$

So, normalized critical load (increment) is defined as Eq. (7).

$$\zeta = \frac{\tilde{\lambda}_c}{C_0 \sigma^{\rho}} = \begin{cases} -\tilde{a} & limit\ point & (\rho = 1) \\ -|\tilde{a}|^{\frac{1}{2}} & asymmetric\ bifurcation\ point & (\rho = \dfrac{1}{2}) \\ -\tilde{a}^{\frac{2}{3}} & symmetric\ bifurcation\ point & (\rho = \dfrac{2}{3}) \end{cases} \tag{7}$$

Thus, the cumulative distribution function, $F_\zeta(\zeta)$, and the reliability function, $R_\zeta(\zeta)$, for normalized critical load are evaluated.

$$F_\zeta(\zeta) = \int_{-\infty}^{\zeta} f_\zeta(\zeta) d\zeta\ ; \quad R_\zeta(\zeta) = 1 - F_\zeta(\zeta) \tag{8}$$

where f_ζ: is the probability density function of ζ. Without expressing further details (more details can be seen in (Ikeda and Murota, 2010; Ikeda et al., 1996; Kiyohiro and Kazuo, 1993)), the mean value $E[\zeta]$ and the variance $Var[\zeta]$ for different types of critical points subjected to the standard normal distribution are as Eq. (9).

$$\begin{cases} limit\ point & \begin{cases} E[\zeta] = 0 \\ Var[\zeta] = 1 \end{cases} \\ Asymmetric\ point\ of\ bifurcation & \begin{cases} E[\zeta] = -0.822 \\ Var[\zeta] = (0.349)^2 \end{cases} \\ symmetric\ point\ of\ bifurcation & \begin{cases} E[\zeta] = -0.802 \\ Var[\zeta] = (0.432)^2 \end{cases} \end{cases} \tag{9}$$

Furthermore, the following equations for the mean and the variance of the ultimate load are computed.

$$E[\lambda_c] = \lambda_c^0 + E[\zeta]C_0\sigma^\rho; \\ Var[\lambda_c] = Var[\zeta](C_0\sigma^\rho)^2 \tag{10}$$

In many cases, it is not applicable to calculate the above-mentioned equations theoretically due to variety of reason such as the high nonlinearity. Thereupon, for finding the $C_0\sigma^\rho$ and λ_c^0, the semi-empirical evaluation procedure is used. In this procedure, for a series of imperfection vector the equilibrium equation is solved and the critical load of structure is obtained. Afterward, the unknown values are computed by substituting the mean and the variance values of sample into the following equations.

$$C_0\sigma^\rho = \begin{cases} (Var_{sample}[\lambda_c])^{1/2} & limit\ point\ (\rho = 1) \\ (Var_{sample}[\lambda_c])^{\frac{1}{2}}/0.349 & asymmetric\ bifurcation\ point\ (\rho = 1/2) \\ (Var_{sample}[\lambda_c])^{\frac{1}{2}}/0.432 & symmetric\ bifurcation\ point\ (\rho = 2/3) \end{cases} \tag{11}$$

$$\lambda_c^0 = \begin{cases} E_{sample}[\lambda_c] & limit\ point \\ E_{sample}[\lambda_c] + 2.35(Var_{sample}[\lambda_c])^{\frac{1}{2}} & asymmetric\ bifurcation\ point\ (\rho = 1/2) \\ E_{sample}[\lambda_c] + 1.86(Var_{sample}[\lambda_c])^{\frac{1}{2}} & symmetric\ bifurcation\ point\ (\rho = 2/3) \end{cases} \tag{12}$$

λ_c^0 is computed by substituting the values obtained from this method into Eq. (10).

Theory for Double Critical Points

In nature, systems typically have group symmetries, therefore, multiple critical points appear in them. In keeping with the general condition of Eq. (1), the equivariance of the equation can be rewritten mathematically to a finite group 'G' as below (Kiyohiro and Kazuo, 1993; Murota and Ikeda, 1992).

$$T(g)\boldsymbol{F}(\lambda, \boldsymbol{u}, \boldsymbol{v}) \\ = \boldsymbol{F}(\lambda, T(g)\boldsymbol{u}, S(g)\boldsymbol{v}), g \in G \tag{13}$$

Again by avoiding further details, the values of $C(\vec{d})$ and ρ in Eq. (4) for different types of critical points are obtained from the following equations.

$$\begin{cases} \rho = \dfrac{2}{3}, & C(\vec{d}) = -C_0.a^{\frac{2}{3}} & if\ \dfrac{n}{m} \geq 5\ and\ unstable \\ \rho = \dfrac{2}{3}, & C(\vec{d}) = C_0.a^{\frac{2}{3}} & if\ \dfrac{n}{m} \geq 5\ and\ stable \\ \rho = \dfrac{1}{2}, & C(\vec{d}) = -\tau(d)C_0.a^{\frac{1}{2}} & if\ \dfrac{n}{m} = 3 \\ \rho = \dfrac{2}{3}, & C(\vec{d}) = -\tau(d)C_0.a^{\frac{2}{3}} & if\ \dfrac{n}{m} = 4 \end{cases} \tag{14}$$

where $\tau(\vec{d})$: is a positive-nonlinear function of $\vec{d}$ and the 'n' indicates the invariance with respect to 'n' rotations and 'n' reflections as well. The 'm' is the greatest common divisor of 'n' and 'j'. The 'j' is a positive number depending on subspace of $\ker((J^0)^T)$. For further details follow the (Ikeda and Murota, 2010; Ikeda et al., 1996; Kiyohiro and Kazuo, 1993).

With introducing the $x = (\frac{a}{\tilde{\sigma}})^2$ where subjected to the exponential distribution (χ^2 distribution of two degrees of freedom) the normalized critical load increment is obtained as Eq. (15).

$$\zeta = \frac{\tilde{\lambda}_c}{C_0\sigma^\rho} = \begin{cases} -x^{\frac{1}{3}} & if\ \dfrac{n}{m} \geq 5\ and\ unstable\ \left(\rho = \dfrac{2}{3}\right) \\ x^{\frac{1}{3}} & if\ \dfrac{n}{m} \geq 5\ and\ stable\ (\rho = \dfrac{2}{3}) \\ -\tau x^{\frac{1}{4}} & if\ \dfrac{n}{m} = 3\ \left(\rho = \dfrac{1}{2}\right) \\ -\tau x^{1/3} & if\ \dfrac{n}{m} = 4\ (\rho = \dfrac{2}{3}) \end{cases} \tag{15}$$

So, by performing some mathematical calculations, the probability density function is calculated for different types of critical points.

$$f_\zeta(\zeta) = \begin{cases} \dfrac{n}{m} \geq 5 & \dfrac{3\zeta^2}{2}\exp\left(\dfrac{-|\zeta|^3}{2}\right) & -\infty < \zeta < 0 \\ \dfrac{n}{m} = 3 & \displaystyle\int_{\tau_{min}}^{\tau_{max}} f_b\left(\frac{|\zeta|}{\tau}\right)\frac{f_\tau(\tau)}{\tau}d\tau & -\infty < \zeta < 0 \\ \dfrac{n}{m} = 4 & numerically\ should\ be\ calculated & \end{cases} \tag{16}$$

The mean $E[\zeta]$ and the variance $Var[\zeta]$ for different types which are subjected to standard normal distribution are explained as Eq. (17), likewise the previous section.

$$\begin{cases} \dfrac{n}{m} \geq 5 & \begin{cases} E[\zeta] = -1.13 \\ Var[\zeta] = (0.409)^2 \end{cases} \\ \dfrac{n}{m} = 3 & \begin{cases} E[\zeta] = 1.91 \\ Var[\zeta] = (0.590)^2 \end{cases} \\ \dfrac{n}{m} = 4 & numerically\ should\ be\ calculated \end{cases} \tag{17}$$

Consequently, semi-empirical equations are calculated in the form of Eq. (18).

$$C_0\sigma^{\rho} = \begin{cases} (Var_{sample}[\lambda_c])^{\frac{1}{2}}/0.409 & n/m \geq 5 \\ (Var_{sample}[\lambda_c])^{\frac{1}{2}}/0.590 & n/m = 3 \end{cases}$$
$$\lambda_c^0 = \begin{cases} E_{sample}[\lambda_c] + 2.75(Var_{sample}[\lambda_c])^{\frac{1}{2}} & n/m \geq 5 \\ E_{sample}[\lambda_c] + 3.24(Var_{sample}[\lambda_c])^{\frac{1}{2}} & n/m = 3 \end{cases} \quad (18)$$

THEORY

As mentioned before, most of specifications and manufacturers documents define imperfection limits (Δ_{max}) as a prescribed value ($|\varepsilon\, d[i]| \leq \Delta_{max}$). Specification numbers of standard deviation can be obtained by using the normal distribution function.

$$S_{max} = \frac{\Delta_{max} - \mu_k}{\sigma_k} \quad (19)$$

where μ_k: is the mean value at any imperfection node k. S_{max}: is the specification numbers of standard deviation. As mentioned before, for each $d[i]$ the mean value, μ_k, is equal to zero, so:

$$S_{max} = \frac{\Delta_{max}}{\sigma_k} \; or \; \sigma_k = \frac{\Delta_{max}}{S_{max}} \quad (20)$$

Table 1 gives the probability of a statistical random variable between –S and S.

Table 1. Probability of statistical random variable

S	P (%)
1.00	68.26
2.00	95.44
3.00	97.74
4.00	99.99

The aim of this paper is to detect the type of bifurcation point and represent the critical load-reliability diagram for shallow lattice domes. For this purpose, the following steps are used for each example.

Step 1: In this step, the initial geometry of the perfect system is formed and the corresponding critical load is calculated by the method of Kani and Heidari (2007). In this method the first critical load, λ_c^0, is obtained using an automatic technique and examining the eigenvalues during the incremental process (Magnusson, 2000). This automatic technique named as automatic perturbed analysis is described in their work in detail (Kani and Heidari, 2007). Finding the critical load of perfect system is the aim of this step. This load is the upper bound of the load which could be carried by the structure.

Step 2: An imperfection vector according to Eq. (2) will be created in this step. For this purpose, σ_k should be determined for each imperfection element. So, in Eq. (20) 'S' is set to 4. It is notable to mention again that the imperfect elements are subject to normal distribution with mean value of zero.

Step 3: The dome which is created in the above-mentioned steps is numerically solved and the corresponding critical load is obtained.

Step 4: Steps 2 and 3 are repeated for a finite series of random imperfection system.

Step 5: At this stage, the average value of critical load of the samples is calculated and compared with the semi-empirical one for various types of critical points. Eq. (21) shows the formula for the mean value which is carried out by semi-empirical method. After determining the mean-value error between the semi-empirical method and samples, type of the bifurcation point is demonstrated.

The following equation for various kinds of critical points can be obtained by performing some simple mathematical operations.

$$E[\lambda_c] = \begin{cases} simple\ critical\ point & \begin{cases} \lambda_c^0 & limit\ point \\ \lambda_c^0 - 0.822\hat{C} & asymmetric\ bifurcation\ point \\ \lambda_c^0 - 0.802\hat{C} & symmetric\ bifurcation\ point \end{cases} \\ double\ critical\ point & \begin{cases} \lambda_c^0 - 1.125\hat{C} & \frac{n}{m} \geq 5 \\ \lambda_c^0 - 1.911\hat{C} & \frac{n}{m} = 3 \end{cases} \end{cases} \quad (21)$$

where $\hat{C} = C_0\sigma^\rho$ and can be obtained by Eq. (11) or (18) based on the point type.

Step 6: In the last step, the histogram and critical load-reliability diagram are established. Furthermore, the safety factor of dome is determined based on semi-empirical method.

RESULTS AND DISCUSSIONS

The purpose of the present work is to bring forward the critical load-reliability diagram by studying the semi-empirical method and detecting the type of critical point for shallow lattice domes. As mentioned earlier using theoretical evaluation for large-scale structures is not applicable. Therefore, using the semi-empirical evaluation procedure is suggested when using the theoretical one is not possible, as is usually the case with high nonlinearity (Kiyohiro and Kazuo, 1993).

To achieve this goal, first, three small tents (Kiyohiro and Kazuo, 1993) have been analyzed to assess the capabilities of the present code. Afterward, two shallow lattice domes with fully-rigid connections (beam-column elements) has been analyzed and the results are presented.

N-Bar Truss Tents

For initial examples three tents with 3-member to 5-member and following geometry (Figure 1) have been analyzed. They are elastic n-bar truss tents (n = 3, 4, 5) which are subjected to a vertical load λ applied to the top node. In perfect system all members have the same modulus of elasticity and same cross-sectional area as E and A, respectively. Accordingly, the equations of n-bar truss tents are $D_n - \text{equivariant}$ (Ikeda et al., 1998). These examples were also used in Murota and Ikeda (1992).

In these examples the imperfection vector is $v = (A_1, \dots, A_p)^T$. In the perfect system, A_i are all the same. Finite Elements solutions for 1000 samples in each example were carried out. Imperfection vectors are subjected to normal distribution of $N(o, \varepsilon^2 I_p)$ and magnitude of $\varepsilon = 10^{-4}$. According to the definition of section "Theory for double critical points" in these examples n/m are 3, 4 and 5, respectively. Therefore, theoretical and semi-empirical probability density functions for n-bar truss tent are as Eqs. (16) and (18).

Consequently, values λ_c^0 and $C_0\sigma^\rho$ can be obtained. It is worth mentioning that the theoretical function is not applicable for the 4-bar truss and the semi-empirical one will be obtained through numerical integration (Kiyohiro and Kazuo, 1993). Theoretical (if applicable), semi-empirical, and histogram results for n-bar truss tents is depicted in Figure 2. As shown in this figure theoretical and empirical functions are in fair agreement with the histogram in each case. The present numerical results in comparison with the results presented by (Kiyohiro and Kazuo, 1993) are in relatively good agreement, as well.

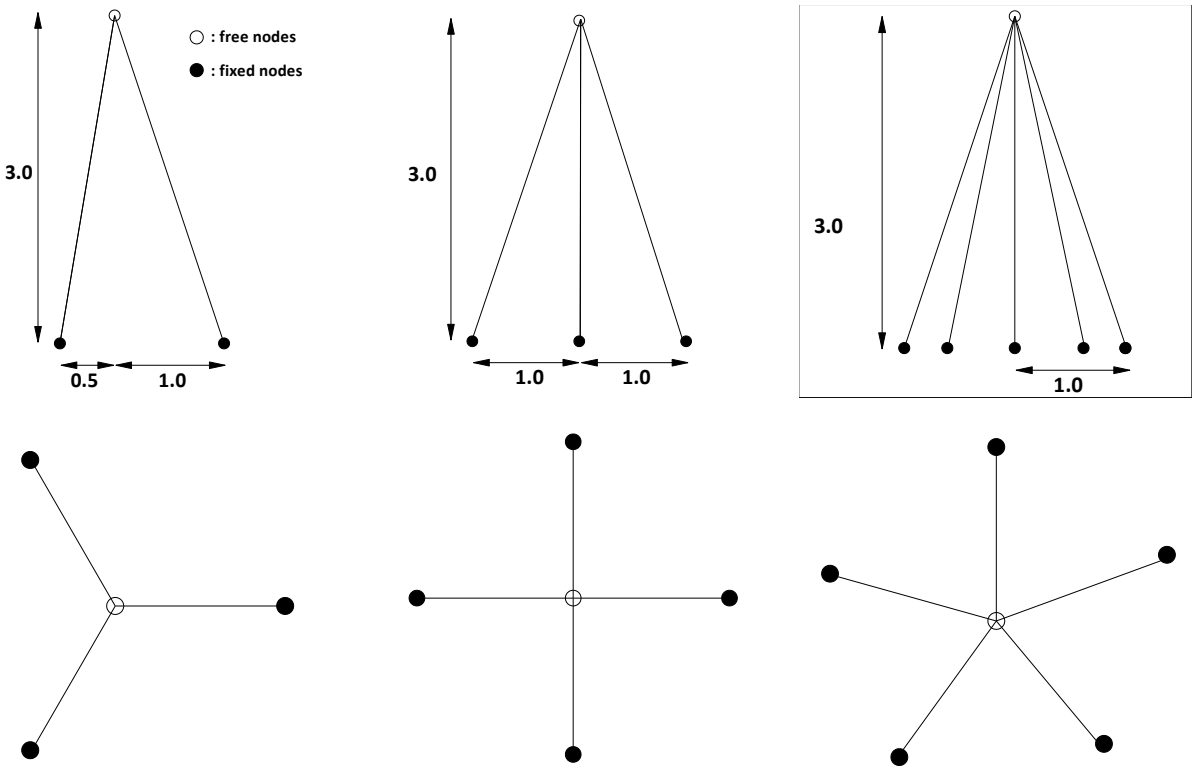

a b c

Fig. 1. Geometry of n-bar truss tents: a) n = 3, b) n = 4, c) n = 5

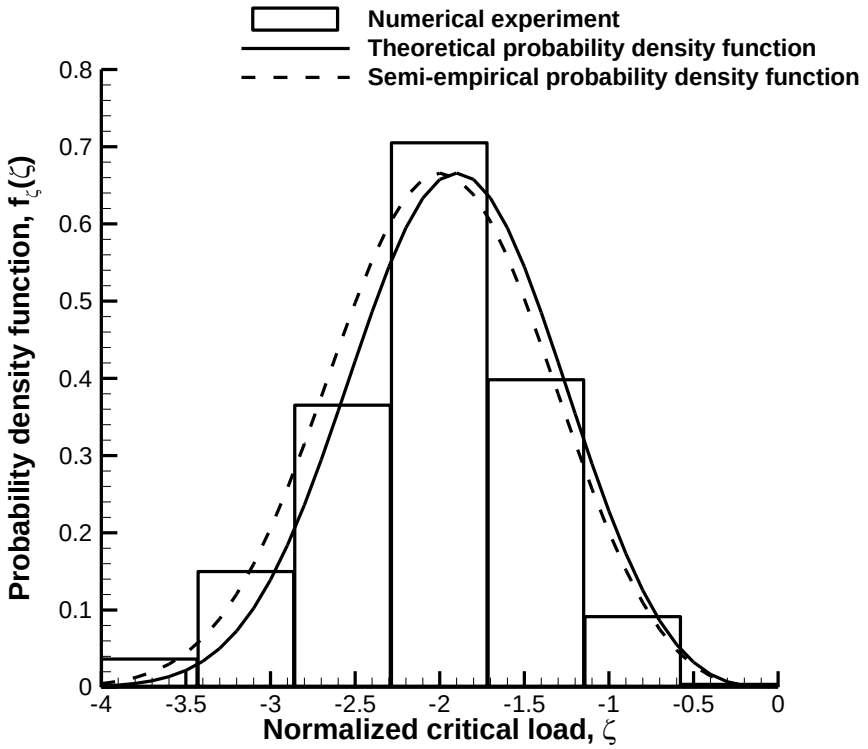

(a) n = 3

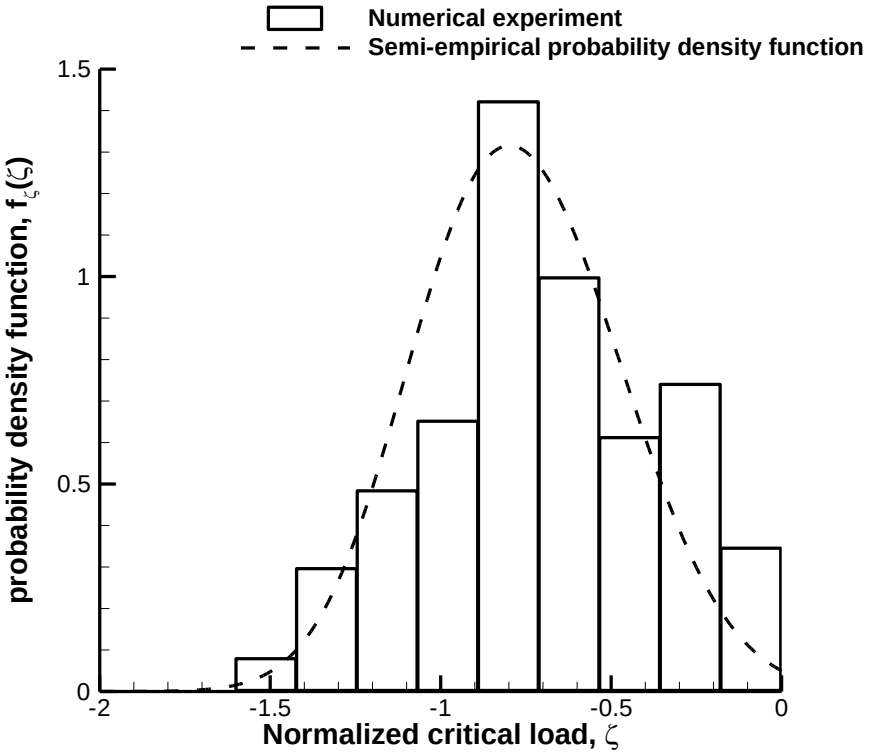

(b) n = 4

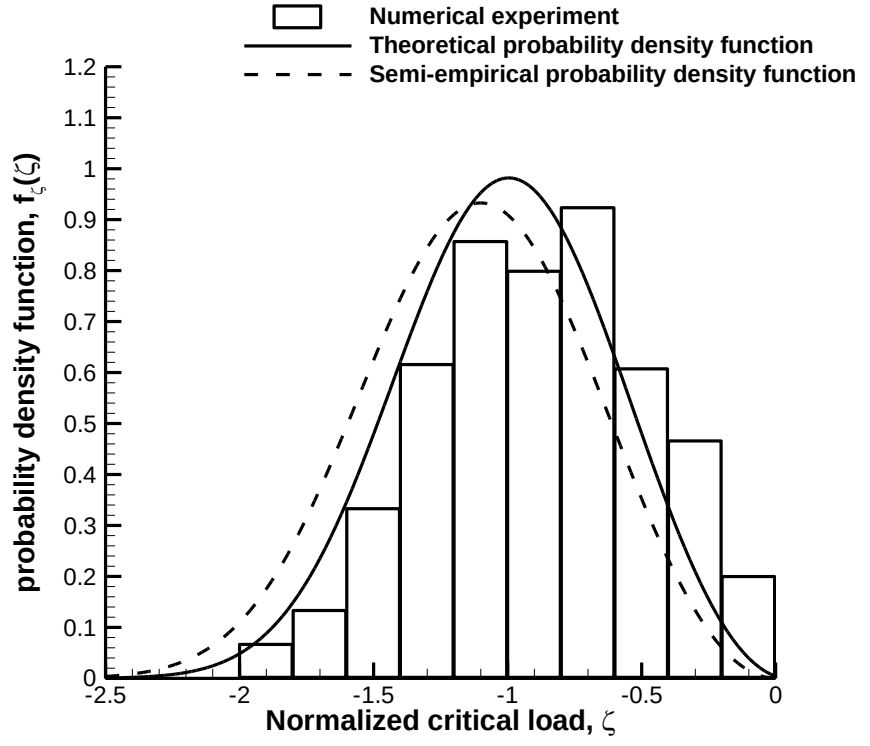

(c) n = 5

Fig. 2. Comparison of theoretical and semi-empirical probability density function and histogram of n-bar truss tents

24-Member Dome

In the next example, a 24-member lattice dome is studied. The undeformed shape of dome is depicted in Figure 4 and theoretical coordinates of nodes are described in Table 2. All joints in this example are assumed fully rigid and a vertical load in –Y direction is applied to the center node. Members are made from steel of square cross-sectional shape with dimensions of 6 mm and material properties which are listed in Table 3.

Table 2. Theoretical coordinates of nodes for 24-member dome

Node number	X (mm)	Y (mm)	Z (mm)
1	0.00	82.16	0.00
2	250.00	62.16	0.00
3	125.00	62.16	-216.50
4	-125.00	62.16	-216.50
5	-250.00	62.16	0.00
6	-125.00	62.16	216.50
7	125.00	62.16	216.50
8	433.00	0.00	-250.00
9	0.00	0.00	-500.00
10	-433.00	0.00	-250.00
11	-433.00	0.00	250.00
12	0.00	0.00	500.00
13	433.00	0.00	250.00

Table 3. Steel properties of domes

Properties	Value	Unit
E	201.81	kN/mm^2
σ_y	0.72±0.14	kN/mm^2
H'	2.21	kN/mm^2

In this example, it is assumed that nodes are at their perfect coordinates and only the section properties and the cross sectional dimensions of members are not perfect. For each member, the dimensions (length and width of sectional area), modulus of elasticity, and yield stress are imperfect. Perfect and imperfect sectional area of members is shown in Figure 3 schematically. It is worthwhile to discuss that the modulus of elasticity does not vary noticeably from sample to sample. Indeed, the deviation of this parameter is small, but yield stress and cross-sectional dimensions' deviations are considerable. So, each member has 3 parameters in imperfection vector and the whole dome have 72 parameters of imperfection. It is noteworthy to remark that the high value of yield stress is probably due to the cold drawing of the material (Kani and Heidari, 2007).

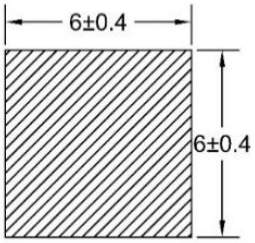

Fig. 3. Perfect and imperfect cross-sectional dimensions (mm)

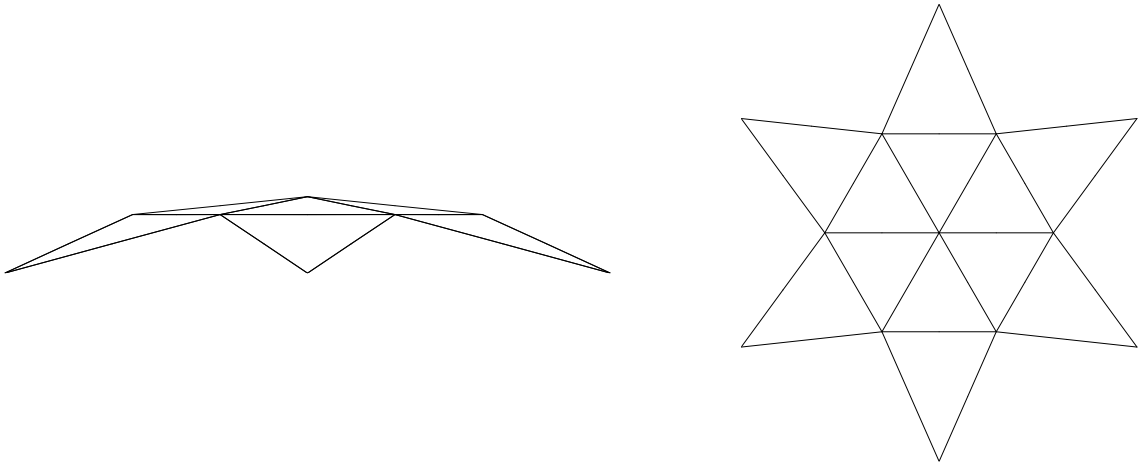

(a) (b)

Fig. 4. a) Plan, b) view of 24-member dome

The Finite Element analysis was performed for the first critical load which is governed by unstable group-theoretic double points of bifurcation. The result for this critical load is 0.728 kN. Afterward, numerical analyses had been performed for 1000 imperfect samples. The minimum and maximum load which are carried out by analyses are 0.714 kN and near to 0.728 kN, respectively. The histogram of numerical results is pictured in Figure 5. However corresponding to the definition of section "Theory for double critical points" $\frac{n}{m} \geq 5$; but for comparison between different types, the value of $\hat{C} = C_0\sigma^\rho$ is calculated. $\hat{C}$ is calculated by assuming limit, asymmetric and Unstable-symmetric for simple critical point, and $\frac{n}{m} \geq 5$ and $\frac{n}{m} = 3$ for double critical point. Then the mean value, $E_{semi-empirical}$, from semi-empirical evaluation procedure is obtained and compared with the mean of samples, $E_{sample} = 0.7206\, kN$, then the relative error is computed. As expected and shown in Table 4, relative error for $\frac{n}{m} \geq 5$ is the least and equal to 0.07%. In Figure 5, in addition to displaying the histogram, semi-empirical curve which has the least relative error is depicted.

Table 4. Comparison of mean value from semi-empirical method and sample for different type of bifurcation point for 24-member dome

Type of bifurcation point		$C_0\sigma^\rho$	$E[\lambda_c]$ (kN)	Error
Simple critical	Limit point	0.0023	0.7276	0.97%
	Asymmetric bifurcation point	0.0067	0.7220	0.20%
	Symmetric bifurcation point	0.0054	0.7232	0.37%
Double critical	$\frac{n}{m} = 3$	0.0040	0.7199	0.09%
	$\frac{n}{m} \geq 5$	0.0058	0.7211	0.07%

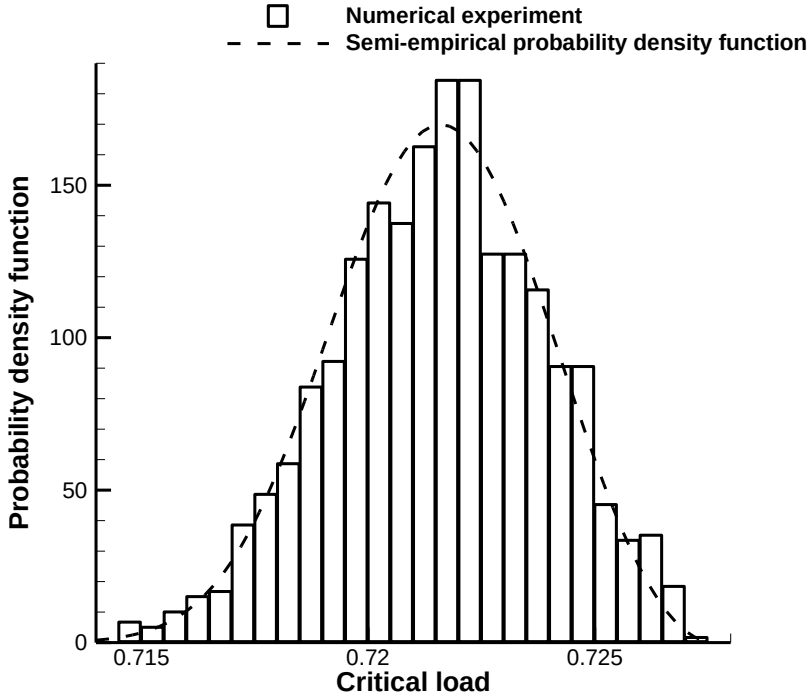

Fig. 5. Comparison of semi-empirical probability density function and histogram for 24-member dome

Real-Size Dome

Compared to the previous examples, this one is a real-size dome with I-shaped section. It has 133 members and 61 nodes. Characteristics of steel I-shaped section are described in Figure 6 and Table 3. Cross-sectional area is A = 2328 mm^2 and moment of inertia about x and y axes are Ix = 14616736 mm^4 and Iy = 1003384 mm^4, respectively. Theoretical geometry of the dome in millimeters is illustrated in Figure 7. Additionally, nine points of integration are used to monitor the spread of plasticity along the section of members. Not only the joints but also support nodes of dome are taken to be fully rigid. Furthermore, a vertical concentrated load on central node is considered in –Z direction.

The result for the first critical load is computed as 591.28 kN by performing the finite element analysis. Then an ensemble of 1000 sets of initial imperfections following the normal distribution was employed and the numerical solution was performed. The minimum and maximum load which were obtained out by analyses are 558 kN and near to 591 kN, respectively. The histogram of numerical results is depicted in Figure 8. The mean value for these sets, E_{sample}, are 572.32 kN. Although n/m is greater than 5, the value of $\hat{C}$ is calculated for comparison. $\hat{C}$ is calculated by assuming limit, asymmetric and Unstable-symmetric for simple critical point, and $\frac{n}{m} \geq 5$ and $\frac{n}{m} = 3$ for double critical point. Afterward, the $E_{semi-empirical}$ is obtained and compared with the E_{sample}, and thereupon relative error is computed. As was predicted and shown in Table 5, relative error for $\frac{n}{m} \geq 5$ is the least and equal to 0.02%. In Figure 8, in addition to displaying the histogram, semi-empirical curve which has the least relative error is presented.

Table 5. Comparison of semi-empirical probability density function and histogram for 24-member dome

Type of bifurcation point	$C_0\sigma^\rho$	$E[\lambda_c]$ (kN)	Error	
Simple critical	Limit point	6.8050	591.19	3.30 %
	Asymmetric bifurcation point	19.4988	575.16	0.50%
	Symmetric bifurcation point	15.7525	578.55	1.09%
Double critical	$\frac{n}{m} = 3$	11.5340	569.15	0.55%
	$\frac{n}{m} \geq 5$	16.6383	572.47	0.02%

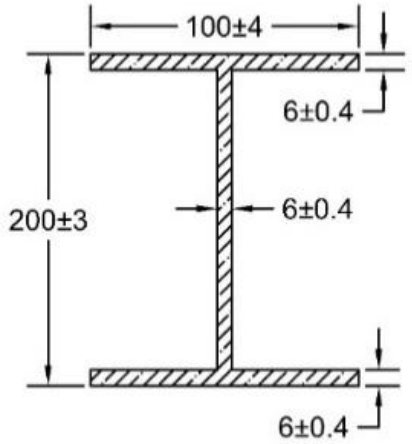

Fig. 6. Perfect and imperfect cross-sectional dimensions (mm) of 133-member dome

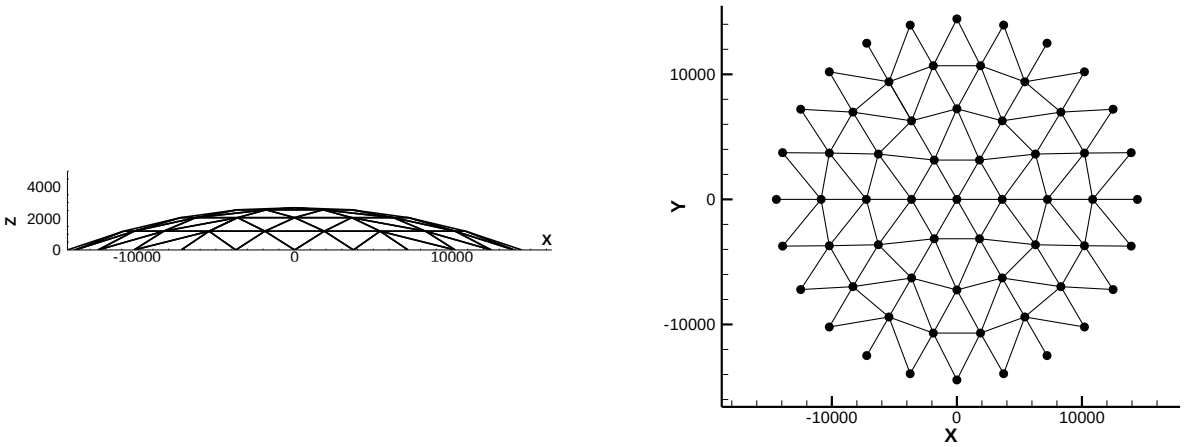

(a) (b)

Fig. 7. a) Plan, b) view of 133-member dome (all dimensions in mm)

As previously noted, finding the worst imperfection pattern (TWIP) is not only difficult but also is uneconomical in many situations. Because the probability of such an event is seldom practical. Using TWIP is recommended only for designing very special structures and using reliability function is sufficient for common structures. The reliability function and the histogram are plotted in Figure 9. Thus, from this figure it can be found that the allowable load is 564 kN for 95% level of confidence. The present analysis shows that using automatic perturbed critical load is not safe enough for shallow lattice domes and reliability function should be brought into play.

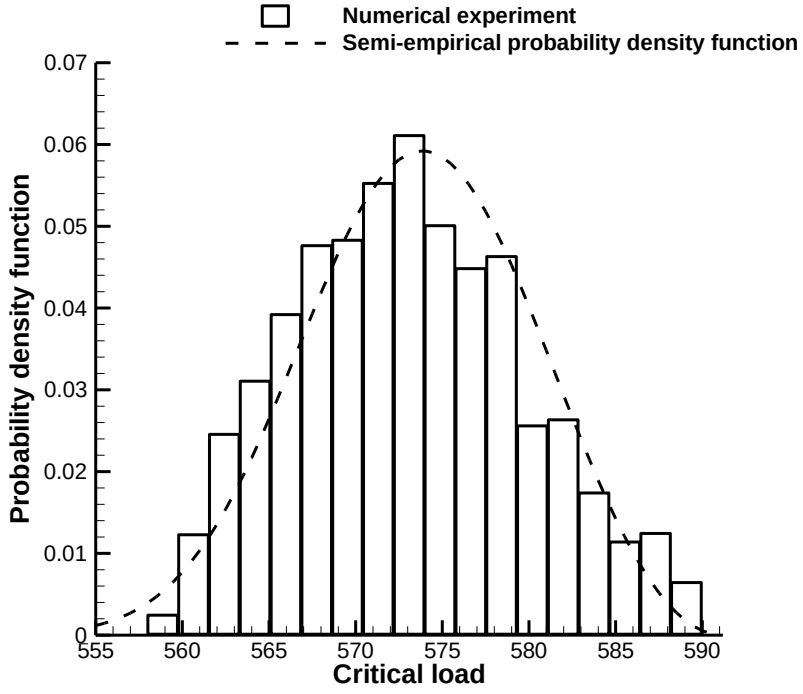

Fig. 8. Comparison of semi-empirical probability density function and corresponded histogram for 133-member dome

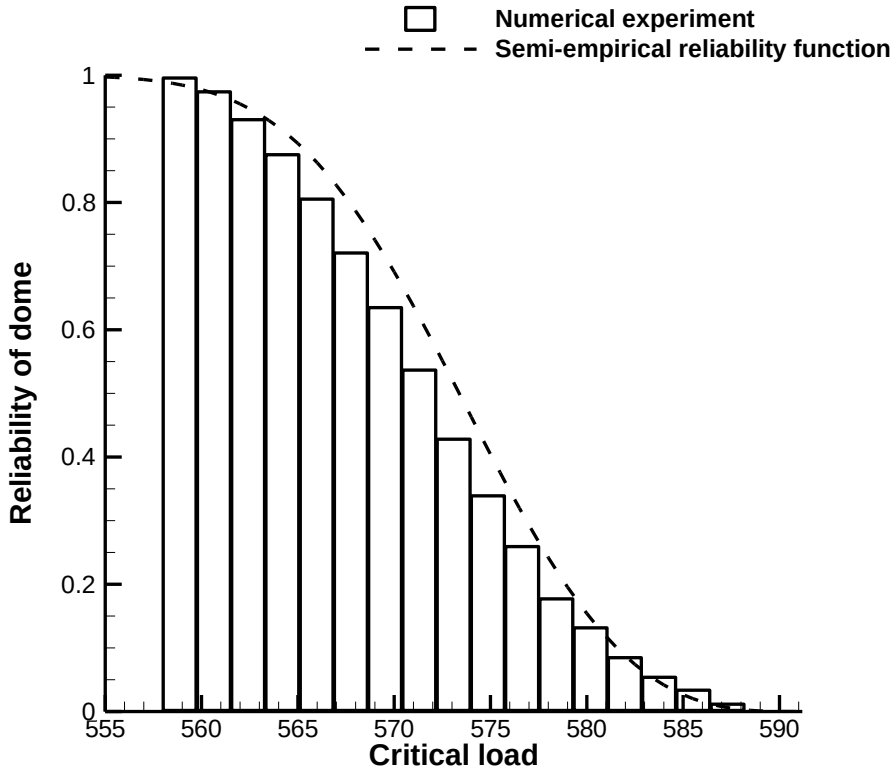

Fig. 9. Comparison of semi-empirical reliability and corresponded histogram for 133-member dome

CONCLUSIONS

The purpose of this paper is to present the reliability function for shallow lattice domes by studying different types of bifurcation. Bifurcation plays a significant role in the safety of structures, albeit this is not systematically reflected in common design rules especially for shallow lattice domes. It is a well-known fact that the material properties and the cross-sectional area are not deterministic. In this light, it shall be pointed out that the critical load and the reliability of dome are influenced by uncertainties.

In this paper after a succinct introduction of previous studies, a review of different types of bifurcation points and governing equations was performed. Afterward, steps of the present method and the probabilistic relationships were stated. For the beginning of examples, as shown in section "n-bar truss tents", three tents which previously had been studied by Murota and Ikeda were analyzed to demonstrate the feature of CNASS. Results of primary examples showed fair agreement with previous studies. Then an example for the domes with rigid-connections was shown in section "24-Member Dome". In this example a 24-member dome was analyzed. The star-shaped dome which was investigated in this section had been treated as exemplary in this field by many researchers. Results presented in this section showed that the semi-empirical evaluation procedure can be used instead of theoretical one without any significant loss in accuracy. Contrary to basic examples, in the last example the reliability of a large-scale dome with I-shaped members was investigated. The results illustrated in this paper highlighted the significance of reliability analysis in shallow lattice domes. They showed that the so-called automatic perturbed analysis is not a safe by itself and other effects of random distribution

of material properties should be taken into account.

The present study was focused on symmetric loads and imperfection in materials as well. Effects of asymmetric loads and also other imperfections will be investigated on further studies. Also seismic loading is a point that was not explored in this work. So as an outlook to further researches, seismic loads can be brought into the model.

As noted earlier, acquiring the worst imperfection pattern not only costs much of run-time on machine but also is inadvisable for commonplace structures. So, designing based on the worst imperfection pattern is preferred for very special structures, because the occurrence of such a pattern during construction is very rare. So in the present work, the critical load-reliability diagram is used to introduce a safety factor. In the last example it was shown that for 95% of confidence level a reduction factor near to 4.5% should be brought into account. This factor should be applied on critical load which is obtained by the automatic perturbed analysis.

As was stated before, the automatic perturbed analysis yields the first critical point on the main path of engineering interest, governing critical load of dome whether this point is simple or double point of bifurcation. Although the automatic perturbed analysis provides a reasonable upper load limit for dome, it does not necessarily represent a reliable estimate of the ultimate load of the structure. This is one of the main outcomes of this paper. So, the authors recommend that a suitable safety factor be applied on the automatic perturbed load or the method utilized in this paper be used to obtain the critical load-reliability diagram.

Another result of this paper is to propose an applicable method for detecting the type of bifurcation point in large scaled domes. Knowing the type of bifurcation point accompanying the reliability diagram can bring a clear insight into design. Finally, shallow domes due to their benefits have been a favorite of designer. Since these structures typically occupy a large area, the safety of these structures must be satisfactorily achieved. So, the present method may aid in finding appropriate values for the safety factor of domes. This goal can be achieved by obtaining the desired level of reliability.

ACKNOWLEDGEMENT

Authors acknowledge the support and fund of the University of Tehran, College of Engineering, School of Civil Engineering for Computer-Aided Study.

REFERENCES

Abatan, A.O. and Holzer, S.M. (1978). "Degree of stability of geodesic domes with independent loading parameters", *Computers and Structures*, 9(1), 43-51.

Akkas, N. (1976). "Bifurcation and snap-through phenomena in asymmetric dynamic analysis of shallow spherical shells", *Computers and Structures*, 6(3), 241-251.

Alvarez, D.A. and Hurtado, J.E. (2014). "An efficient method for the estimation of structural reliability intervals with random sets, dependence modeling and uncertain inputs", *Computers and Structures*, 142, 54-63.

Fröderberg, M. and Thelandersson, S. (2015). "Uncertainty caused variability in preliminary structural design of buildings", *Structural Safety*, 52, 183-193.

Ghassemieh, M. and Badrkhani Ajaei, B. (2018). "Impact of Integration on Straining Modes and Shear-Locking for Plane Stress Finite Elements", *Civil Engineering Infrastructures Journal*, 51(2), 425-443.

Hassan, M.M. (2013). "Optimization of stay cables in cable-stayed bridges using finite element, genetic algorithm, and B-spline combined technique", *Engineering Structures*, 49, 643-654.

Heidari, A., Karimi, H. and Mahmoudzadeh Kani, I. (2019). "Collapse of reticulated domes, a case study of Talakan oil tank", *Scientia Iranica*, (in press).

Hurtado, J.E. and Alvarez, D.A. (2013). "A method for enhancing computational efficiency in Monte Carlo calculation of failure probabilities by

exploiting form results", *Computers and Structures*, 117, 95-104.

Ikeda, K. and Murota, K., (2010). *Imperfect bifurcation in structures and materials: Engineering use of group-theoretic bifurcation theory*, Springer Science and Business Media.

Ikeda, K., Murota, K. and Elishakoff, I. (1996). "Reliability of structures subject to normally distributed initial imperfections", *Computers and Structures*, 59(3), 463-469.

Ikeda, K., Murota, K., Maruyama, K. and Yasunami, H. (1998). "Uncertainty in the strength of materials and structures", *Computers and Structures*, 67(1), 71-82.

Jensen, H.A., Mayorga, F. and Papadimitriou, C. (2015). "Reliability sensitivity analysis of stochastic finite element models", *Computer Methods in Applied Mechanics and Engineering*, 296, 327-351.

Kamiński, M. and Świta, P. (2015). "Structural stability and reliability of the underground steel tanks with the Stochastic Finite Element Method", *Archives of Civil and Mechanical Engineering*, 15(2), 593-602.

Kani, I.M. and Heidari, A. (2007). "Automatic two-stage calculation of bifurcation path of perfect shallow reticulated domes", *Journal of Structural Engineering*, 133(2), 185-194.

Karimi, H. and Kani, I.M. (2019). "Finding the worst imperfection pattern in shallow lattice domes using genetic algorithms", *Journal of Building Engineering*, 23, 107-113.

Keshtegar, B .and Miri, M. (2013). "An enhanced HL-RF method for the computation of structural failure probability based on Relaxed approach", *Civil Engineering Infrastructures Journal*, 46(1), 69-80.

Kitipornchai, S. and Al-Bermani, F.G.A. (1992). "Nonlinear analysis of lattice structures", *Journal of Constructional Steel Research*, 23(1), 209-225.

Kiyohiro, I. and Kazuo, M. (1991). "Random initial imperfections of structures", *International Journal of Solids and Structures*, 28(8), 1003-1021.

Kiyohiro, I. and Kazuo, M .(1993). " Statistics of normally distributed initial imperfections", *International Journal of Solids and Structures*, 30(18), 2445-2467.

Koiter, W.T. (1970). "The stability of elastic equilibrium", Department of Aeronautics and Astronautics, Stanford University, C.A., U.S.A.

Liu, H., Zhang, W. and Yuan, H. (2016). "Structural stability analysis of single-layer reticulated shells with stochastic imperfections", *Engineering Structures*, 124, 473-479.

Liu, W. and Ye, J. (2014). "Collapse optimization for domes under earthquake using a genetic simulated annealing algorithm", *Journal of Constructional Steel Research*, 97, 59-68.

Magnusson, A. (2000). "Treatment of bifurcation points with asymptotic expansion", *Computers and Structures*, 77(5), 475-484.

Meimand, V.Z. and Schafer, B.W. (2014). "Impact of load combinations on structural reliability determined from testing cold-formed steel components", *Structural Safety*, 48, 25-32.

Moghaddasie, B. and Stanciulescu, I. (2013). "Direct calculation of critical points in parameter sensitive systems", *Computers and Structures*, 117, 34-47.

Murota, K. and Ikeda, K. (1992). "On random imperfections for structures of regular-polygonal symmetry", *SIAM Journal on Applied Mathematics*, 52(6), 1780-1803.

Nie, G-.B., Zhi, X.-D., Fan, F. and Dai, J.-W. (2014). "Seismic performance evaluation of single-layer reticulated dome and its fragility analysis", *Journal of Constructional Steel Research*, 100, 176-182.

Radoń, U. (2015). "Numerical aspects of application of FORM in node snapping truss structures", *Archives of Civil and Mechanical Engineering*, 15(1), 262-271.

Ramalingam, R. and Jayachandran, S.A. (2015). "Postbuckling behavior of flexibly connected single layer steel domes", *Journal of Constructional Steel Research*, 114, 136-145.

Taras, A. and Huemer, S. (2015) "On the influence of the load sequence on the structural reliability of steel members and frames", *Structures*, 4, 91-104.